

## EVOLUTION OF GROUND-STATE NUCLEAR SHAPES IN TUNGSTEN NUCLEI IN TERMS OF INTERACTING BOSON MODEL

A. M. Khalaf<sup>a</sup>, A. O. El-Shal<sup>b</sup>, M. M. Taha<sup>b,1</sup>, M. A. El-Sayed<sup>b</sup>

<sup>a</sup> Physics Department, Faculty of Science, Al-Azhar University, Cairo

<sup>b</sup> Mathematics and Theoretical Physics Department, Nuclear Research Center,  
Atomic Energy Authority, Cairo

The tungsten nuclei  $^{180-190}\text{W}$  are investigated within the framework of the interacting boson model using an intrinsic coherent state formalism. The Hamiltonian operator contains only multipole operators of the subalgebra associated with the dynamical symmetries  $SU(3)$  and  $O(6)$ . The study includes the behavior of potential energy surfaces (PESs) and critical points in the space of the model parameters to declare the geometric character of the tungsten isotopic chain. Some selected energy levels and reduced  $E2$  transition probabilities  $B(E2)$  for each nucleus are calculated to adjust the model parameters by using a computer code PHINT and simulated computer fitting program to fit the experimental data with the IBM calculation by minimizing the root-mean-square deviations. The  $^{180-190}\text{W}$  isotopes lie in shape transition  $SU(3)$ – $O(6)$  region of the IBM such that the lighter isotopes come very close to the  $SU(3)$  limit, while the behavior ones tend to be near the  $\gamma$ -unstable  $O(6)$  limit.

В работе исследуются ядра вольфрама  $^{180-190}\text{W}$  в рамках модели взаимодействующих бозонов на основе формализма истинного когерентного состояния. Гамильтониан содержит только мультипольные операторы субалгебры, отвечающей симметриям  $SU(3)$  и  $O(6)$ . Рассматривается поведение поверхностей потенциальной энергии (ППЭ) и критических точек в пространстве модельных параметров, и показывается геометрический характер изотопической цепочки вольфрама. Модельные параметры находятся из описания некоторых выбранных уровней энергии и приведенных  $E2$ -вероятностей перехода  $B(E2)$  для каждого из рассматриваемых ядер. Для этого используется компьютерный код PHINT и симуляция с помощью программы фитирования экспериментальных данных минимизацией среднеквадратичных отклонений. Из результатов компьютерной симуляции цепочки изотопов  $^{180-190}\text{W}$  видно, что более легкие изотопы тяготеют в пределе к симметрии  $SU(3)$ , в то время как  $\gamma$ -нестабильные ядра находятся в пределе  $O(6)$ .

PACS: 01.30.-y; 01.30.Ww; 01.30.Xx

### INTRODUCTION

The interacting boson model (IBM) [1] made a great success in a phenomenological but unified description of quadrupole collective states in even–even nuclei. The basic assumption of the simplest original versions of the IBM is that the nucleus is built on closed shells or inert core with even number of bosons and valance bosons outside the closed shell with angular

---

<sup>1</sup>E-mail: mahmoudmt@hotmail.com

momentum  $L = 0$  and  $L = 2$  called  $s$  and  $d$  bosons analogously to the shell model technique. In the original form of the model known as IBM-1 no distinction is made between proton bosons and neutron bosons.

The IBM is in connection not only with the shell model but also with the collective model [2]. In collective model the deformation of the nuclear surface is respected by five parameters from which a Hamiltonian of a five-dimensional oscillator results. It contains five-fold generating and annihilating operators for oscillator quanta. The operators of these bosons correspond to the operators of the  $d$ -shell in the IBM. The corresponding symmetry group of the IBM is  $U(6)$  and possesses three dynamical symmetry limits, namely  $U(5)$ ,  $SU(3)$ , and  $O(6)$ , which describe vibrational, axially deformed, and gamma-soft nuclei, respectively. It is known that shape phase transition is one of the most significant topics in nuclear structure research. A number of evidence of nuclear shape phase transitions were observed.

Within the IBM, the three symmetry limits are usually represented as vertices of Casten triangle [3]. Shape phase transitions between these vertices were widely studied along several isotopic chains [1, 4, 5] with respect to the vibration of the total number of bosons. It is known that the phase transition  $U(5)$  to  $O(6)$  is second order, while any other transitions within Casten triangle from a spherical to deformed shape are first order [6, 7], since the discovery of critical point symmetries  $E(5)$  [8] and  $X(5)$  [9] which corresponds to the shape transitions from spherical vibrator to gamma-soft rotor ( $U(5)$ – $O(6)$ ) [10–14] and the transition from spherical to axially deformed ( $U(5)$ – $SU(3)$ ) [15–18], respectively.

In addition, the  $Y(5)$  symmetry [19] was introduced to describe the critical point between axial and triaxial deformed shapes. Furthermore, the critical point symmetry  $Z(s)$  was introduced [20] for the prolate to oblate shape phase transition. The doubly even mass tungsten isotopes have been previously investigated both theoretically and experimentally in recent years. The energy levels, electric quadrupole transition probability  $B(E2)$  values of  $^{182-186}\text{W}$  isotopes have been studied within the framework of the IBM-1 [21, 22] and IBM-2 [23]. The aim of the present paper is to investigate the  $SU(3)$ – $O(6)$  shape transition in even–even tungsten isotopes.

The main purpose of the present paper is to study the nuclear shape phase transition from a spherical axially prolate rotor to  $\gamma$ -soft rotor and investigate this transition in even–even tungsten isotopes. Since the IBM has been shown to be quite a good approximation to describe the observed nuclear excitation energies and nuclear shapes, we used the IBM with intrinsic coherent state formalism. The paper is organized as follows. In Sec. 1, the IBM Hamiltonian operator and the intrinsic coherent state are described. Section 2 is devoted to study of the PESs of the IBM Hamiltonian. In Sec. 3, the PESs are analyzed in relation to the critical points. In Sec. 4, the dependence of the shape phase transition on the energy ratios and  $B(E2)$  transition rates are studied. We performed the  $SU(3)$ – $O(6)$  calculations applied to tungsten isotopes in Sec. 5. The final section states the conclusions.

## 1. THE HAMILTONIAN OPERATOR AND THE INTRINSIC COHERENT STATE OF THE IBM-1

In order to study the shape phase transitions in the IBM, a Hamiltonian with one- and two-body terms in the  $sd$  space can be written in three terms of multipole operators in the form [1, 3]

$$H_{\text{IBM}} = a_0 \hat{P}^\dagger \cdot P + a_1 \hat{L} \cdot \hat{L} + a_2 \hat{Q}^X \cdot \hat{Q}^X, \quad (1)$$

where  $a_0$ ,  $a_1$ , and  $a_2$  are the model parameters. Here  $\hat{P}^\dagger$ ,  $\hat{L}$ , and  $\hat{Q}^\chi$  are the pairing, angular momentum, and quadrupole operators, respectively. The explicit form of each multipole operator is defined by the following equations:

$$\hat{P}^\dagger = \frac{1}{2}(d^\dagger \cdot d^\dagger - s^\dagger \cdot s^\dagger), \quad (2)$$

$$\hat{L} = \sqrt{10}[d^\dagger \times d^\dagger]^{(1)}, \quad (3)$$

$$\hat{Q}^\chi = [s^\dagger \times \tilde{d} + d^\dagger \times \tilde{s}]^{(2)} + \chi[d^\dagger \times \tilde{d}]^{(2)}. \quad (4)$$

Here  $s^\dagger$  and  $d^\dagger$  are creation operators of the  $s$  and  $d$  bosons, and  $\tilde{d}$  is the annihilation operator of the  $d$  boson with the time reversal phase with the phase relation

$$\tilde{d}_{2,k} = (-1)^{2+k} d_{2,-k}. \quad (5)$$

Equation (1) defines an IBM-1 Hamiltonian in terms of four independent parameters  $a_0$ ,  $a_1$ ,  $a_2$ , and  $\chi$ .

The general state of a nucleus with  $N$  bosons can be expressed by a boson intrinsic coherent state introduced by Ginocchio and Kirson [24] in the form

$$|c\rangle = \frac{1}{\sqrt{N!}}(\Gamma_c^\dagger)^N |0\rangle, \quad (6)$$

where  $|0\rangle$  stands for the boson vacuum (inert core), and  $\Gamma_c^\dagger$  is the creation operator

$$\Gamma_c^\dagger = \frac{1}{\sqrt{1+\beta^2}} \left[ s^\dagger + \beta \cos \gamma d_0^\dagger + \frac{1}{\sqrt{2}} \beta \sin \gamma (d_2^\dagger + d_{-2}^\dagger) \right]. \quad (7)$$

The deformations  $\beta \geq 0$  and  $\gamma \leq \pi/3$  determine the geometry of nuclear surface.

To investigate the shape phase structure and its transition among the yrast band, we carry out the technique of angular momentum projection [25]. After some derivation, the expectation values of the three multipole operators appearing in Eq. (1) are:

$$\langle c | \hat{P}^\dagger \cdot \hat{P} | c \rangle = \frac{N(N-1)}{4(1+\beta^2)} (1-\beta^2)^2, \quad (8)$$

$$\langle c | \hat{L} \cdot \hat{L} | c \rangle = \frac{6N}{1+\beta^2} \beta^2, \quad (9)$$

$$\begin{aligned} \langle c | \hat{Q}^\chi \cdot \hat{Q}^\chi | c \rangle = & \frac{N}{1+\beta^2} [5 + (1+\chi^2)\beta^2] + \\ & + \frac{N(N-1)}{(1+\beta^2)^2} \left[ 4\beta^2 - 4\sqrt{\frac{2}{7}} \chi\beta^3 \cos 3\gamma + \frac{2}{7}\chi^2\beta^4 \right]. \end{aligned} \quad (10)$$

## 2. THE POTENTIAL ENERGY SURFACES (PESs)

The shape phase transition analysis of the Hamiltonian (1) yields the bosonic PES dependence on  $N$ ,  $\beta$ , and  $\gamma$ . It is represented by the expectation value of the total Hamiltonian in the intrinsic coherent state:

$$E(N, \beta, \gamma) = \langle c | \hat{H} | c \rangle. \quad (11)$$

Using the above expectation values of the multipole operators, Eqs. (8)–(10) yield

$$E(N, \beta, \gamma) = \frac{A_2\beta^2 + A_3\beta^3 \cos 3\gamma + A_4\beta^4}{(1 + \beta^2)^2} + A_0, \quad (12)$$

where the coefficients  $A_2$ ,  $A_3$ ,  $A_4$ , and  $A_0$  are linear combination of the proposed model parameters  $a_0$ ,  $a_1$ ,  $a_2$ , and  $\chi$

$$A_2 = [-(N - 1)a_0 + 6a_1 + (\chi^2 - 8 + 4N)a_2] N, \quad (13)$$

$$A_3 = -4\sqrt{\frac{2}{7}}\chi a_2(N - 1)N, \quad (14)$$

$$A_4 = \left[ 6a_1 + \left( \frac{2N + 5}{7} \chi^2 - 4 \right) a_2 \right] N, \quad (15)$$

$$A_0 = \left[ \frac{1}{4}a_0(N - 1) + 5a_2 \right] N. \quad (16)$$

### 3. LOCATION OF CRITICAL POINTS

The shape of nucleus is defined through the equilibrium value of the deformation parameters  $\beta$  and  $\gamma$ , which are obtained by minimizing  $E(N, \beta, \gamma)$ . A spherical nucleus has a global minimum in the energy surface at  $\beta = 0$ , while a deformed one has the absolute minimum at finite values of  $\beta$ . The parameter  $\gamma$  represents the departure from axial symmetry  $\gamma = 0$ , and  $\gamma = \pi/3$  stands for an axially deformed nucleus prolate and oblate, respectively, while any other value corresponds to a triaxial shape. If the energy surface is independent of  $\gamma$  but shows a minimum at finite value of  $\beta$ , then the nucleus is  $\gamma$ -unstable. The equilibrium value of the deformation parameter  $\beta_0$  is determined by equating the first-order derivative of the PES with respect to  $\beta$  to zero, which leads to the following equation:

$$2A_2 + 3A_3\beta + (4A_4 - 2A_2)\beta^2 - A_3\beta^3 = 0. \quad (17)$$

Also, the phase transition is signaled by the condition at  $\beta = 0$  which fixes the critical points. The location of the critical point can be readily obtained by putting  $d^2E(N, \beta, \gamma)/d\beta^2 = 0$  at  $\beta = 0$ . The condition leads to  $A_2 = 0$ .

1. For pure  $SU(3)$  ( $\chi = -\sqrt{7}/2$ , only quadrupole term) and if we eliminate the contributions of the one-body terms of the quadrupole–quadrupole interaction, the model parameters become

$$A_2 = 4a_2(N - 1)N, \quad (18)$$

$$A_3 = 2\sqrt{2}a_2(N - 1)N, \quad (19)$$

$$A_4 = \frac{1}{2}a_2(N - 1)N. \quad (20)$$

Then the equilibrium equation becomes

$$4 + 3\sqrt{2}\beta - 3\beta^2 - \sqrt{2}\beta^3 = 0, \quad (21)$$

which gives  $\beta = \sqrt{2}$ .

Now we are looking for the value  $a_2$  which produces sufficiently deep minimum at  $\beta = \sqrt{2}$ . At  $\beta = \sqrt{2}$  a deep  $V$  of the deformed minimum is determined in

$$V = [E(N, \beta)_{\beta=0} - E(N, \beta)_{\beta=\sqrt{2}}] = (7 - 2N)Na_2. \tag{22}$$

2. For pure  $O(6)$  ( $\chi = 0$ , only the pairing term), the parameters of the PESs become

$$A_2 = -(N - 1)a_0, \tag{23}$$

$$A_3 = A_4 = 0, \tag{24}$$

$$A_0 = \frac{1}{4}(N - 1)a_0, \tag{25}$$

and the equilibrium equation becomes

$$1 - \beta^2 = 0, \tag{26}$$

which yields  $\beta = 1$ .

To produce a deformed  $\gamma$ -unstable structure, it is of course necessary to exclude terms in  $\cos 3\gamma$  and shift the minimum in  $E(\beta)$  to finite deformation. This can be accomplished by a balance between a negative  $A_2$  term and a larger positive  $A_4$  term. This  $\gamma$ -unstable potential gives predictions shown in the right of Fig. 1. For symmetric prolate rotor, the defined minimum in  $\beta$  requires  $A_3 < 0$  and  $A_3 \gg A_2, A_3 \ll A_4$ .

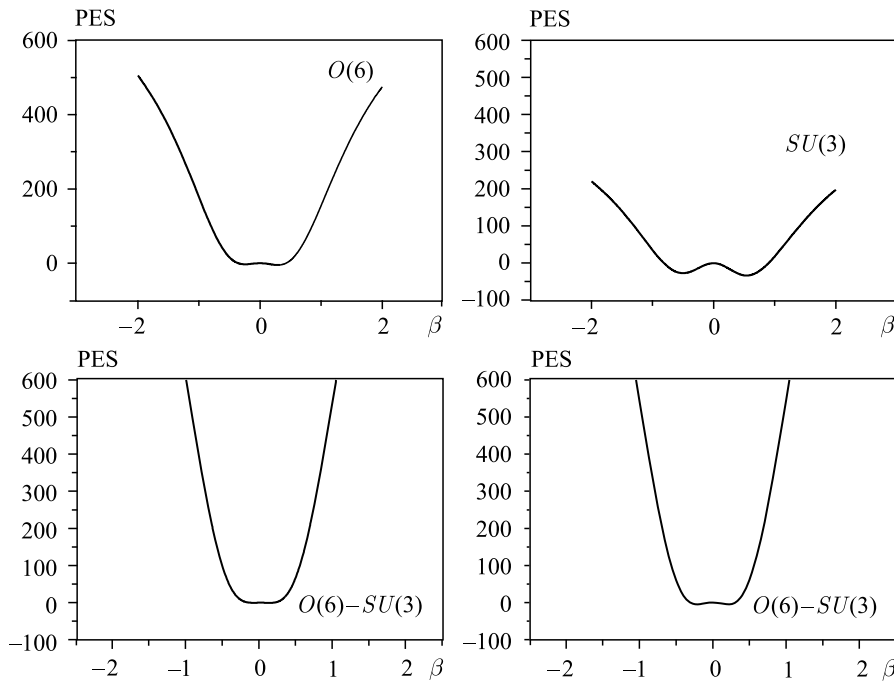


Fig. 1. PES's  $E(\beta)$  plots. The upper left panel shows  $\gamma$ -unstable  $O(6)$ , while the upper right panel denotes a typical rotor  $SU(3)$ . The two lower panels show intermediate transition structure  $O(6)-SU(3)$

3. To describe the transition from axial symmetric deformation to  $\gamma$ -unstable  $SU(3)$ - $O(6)$ , we will consider three cases.

*Case 1.* If  $a_1 = (3/8)a_2$  and  $\chi$  is fixed at  $-\sqrt{7}/2$ , the essential structure changes depending only on  $a_0/a_2 = \lambda$ . To find the inflection point, we put  $A_2 = 0$ , to yield  $\lambda_c = 4$ . If  $a_0/a_4 < \lambda_c$  the behavior is  $SU(3)$ , while if  $a_0/a_4 > \lambda_c$  the behavior is  $O(6)$ .

*Case 2.* If  $a_0 = 0$  and varying the value of the parameter  $\chi$  between  $-\sqrt{7}/2$  and zero.

*Case 3.* This can be described by using a simple quadrupole-quadrupole Hamiltonian and varying  $\chi$  between the limiting values of  $SU(3)$  and  $O(6)$ .

#### 4. $E2$ TRANSITION ENERGY AND $B(E2)$ RATIOS

The electric quadrupole transition operator provides more stringent test of the model. The most general  $E2$  transition operator in the IBM is given by [26]

$$T(E2) = \alpha_2[d^\dagger \tilde{s} + s^\dagger \tilde{d}]^{(2)} + \beta_2[d^\dagger \tilde{d}]^{(2)}, \quad (27)$$

and the reduced electric quadrupole transition probabilities are given by

$$B(E2, I_i \rightarrow I_f) = \frac{1}{2I_i + 1} |\langle I_f || T(E2) || I_i \rangle|^2, \quad (28)$$

where  $I_i$  and  $I_f$  are the angular momenta for the initial and final states, respectively.

The coefficient  $\alpha_2$  being the boson effective charge is an overall scaling factor for all  $B(E2)$  values which is determined from the fit to the experimental  $B(E2, 2_1^+ \rightarrow 0_1^+)$  value. The coefficient  $\beta_2$  may be determined from the quadrupole moment  $Q(2_1^+)$ . The ratio  $\beta_2/\alpha_2 = \chi = -\sqrt{7}/2$  in the  $SU(3)$  limit and is reduced to zero in the  $O(6)$  limit.

The useful quantities of interest which are known to be able to characterize the low-lying energy spectrum and signal the shape phase transition well are the energy ratios  $R$  and the ratios of the  $E2$  transition rates  $B$  defined as

$$\begin{aligned} R_{42} &= \frac{E(4_1)}{E(2_1)}, & R_{62} &= \frac{E(6_1)}{E(2_1)}, & R_{02} &= \frac{E(0_2)}{E(2_1)}, \\ R_{22} &= \frac{E(2_2)}{E(2_1)}, & R_{60} &= \frac{E(6_1)}{E(0_2)}, & \text{with } E(0_1) &= 0, \end{aligned} \quad (29)$$

$$\begin{aligned} B_{42} &= \frac{B(E2; 4_1 \rightarrow 2_1)}{B(E2; 2_1 \rightarrow 0_1)}, & B_{64} &= \frac{B(E2; 6_1 \rightarrow 4_1)}{B(E2; 2_1 \rightarrow 0_1)}, \\ B_{02} &= \frac{B(E2; 0_2 \rightarrow 2_1)}{B(E2; 2_1 \rightarrow 0_1)}, & B_{22} &= \frac{B(E2; 2_2 \rightarrow 2_1)}{B(E2; 2_1 \rightarrow 0_1)}. \end{aligned} \quad (30)$$

For  $SU(3)$ :

$$R_{42} = \frac{10}{3}, \quad R_{02} = \frac{4}{3}(2N - 1), \quad (31)$$

$$B_{42} = \frac{10}{7} \frac{(N-1)(2N+5)}{N(2N+3)} \rightarrow \frac{10}{7}. \quad (32)$$

For  $O(6)$ :

$$R_{42} = \frac{5}{2}, \quad R_{02} = (N - 1), \quad (33)$$

$$B_{42} = \frac{10(N-1)(N+5)}{7(N)(N+4)} \rightarrow \frac{10}{7}. \quad (34)$$

## 5. APPLICATION TO EVEN-EVEN TUNGSTEN NUCLEI

The values of the parameters in the Hamiltonian are obtained for each nucleus in the isotopic chain  $^{180-190}\text{W}$  by using the computer code PHINT [27] and simulated computer fitting program to fit energy levels and  $B(E2)$  transitions of the lowest ground,  $\beta$  and  $\gamma$  bands to the experimental data [28]. The best fit parameters are listed in Table 1 and the calculated energies and  $B(E2)$  ratios are given in Table 2 compared to values of [22] and to the experimental ones, a good agreement is reached. The boson effective charge is taken to be  $\chi$  for all isotopes.

In Fig. 2, we see the evolution of the axial PESs for W isotopes obtained from the IBM Hamiltonian of Eq. (1) as a function of the deformation parameter  $\beta$ . The chain of  $^{180-190}\text{W}$  isotopes is considered as example of  $SU(3)$ - $O(6)$  shape transitions occurring in this mass

**Table 1. The values of the adopted parameters (in MeV) of the present model for the tungsten isotopic chain  $^{180-190}\text{W}$**

Isotope	$N_\beta$	$A_0$	$A_2$	$A_3$	$A_4$
$^{180}\text{W}$	14	1.5456	-18.6929	-7.1038	0.1440
$^{182}\text{W}$	13	1.3604	-17.3568	-6.5964	0.1346
$^{184}\text{W}$	12	0.8268	-10.7827	-4.2823	0.5765
$^{186}\text{W}$	11	0.5373	-7.2426	-3.0365	0.8115
$^{188}\text{W}$	10	0.3418	-4.7203	-2.1739	1.0450
$^{190}\text{W}$	9	0.1390	-1.0943	-1.0447	1.6779

**Table 2. Calculated values of interested energy and  $B(E2)$  ratios characterize the low-lying spectrum in tungsten isotopes  $^{182-186}\text{W}$  compared to the predictions of  $O(6)$  and  $SU(3)$ , [22] and the experimental data**

Cal./Exp.	$R_{42}$	$R_{62}$	$R_{02}$	$R_{60}$	$B_{42}$	$B_{64}$	$B_{22}$	
$SU(3)$	3.33	7	13.7	0.29	1.4	1.48	0	
$^{182}\text{W}$ :	Cal. (present)	3.310	6.950	11.700	0.594	1.411	1.518	0.068
	Cal. ([22])	3.310	6.944	11.190	0.621	1.419	1.520	0.067
	Exp.	3.290	6.800	11.350	0.599	1.380	1.523	0.077
$^{184}\text{W}$ :	Cal. (present)	3.218	6.590	8.590	0.767	1.427	1.549	0.107
	Cal. ([22])	3.218	6.589	8.536	0.772	1.463	1.635	0.103
	Exp.	3.279	6.738	9.018	0.747	1.430	1.357	0.069
$^{186}\text{W}$ :	Cal. (present)	3.098	6.204	6.196	1.001	1.435	1.566	0.189
	Cal. ([22])	3.097	6.203	6.049	1.020	1.443	1.566	0.172
	Exp.	3.245	6.631	7.237	0.916	1.774	2.294	0.125
$O(6)$	2.5	4.5	4.5	1	1.38	1.32	1.38	

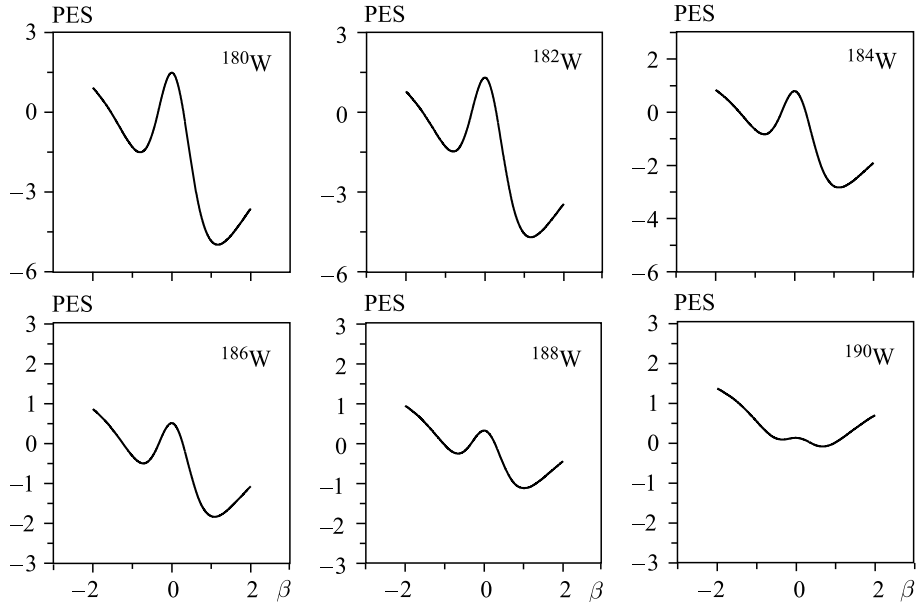


Fig. 2. PESs for  $^{180-190}\text{W}$  ( $N = 14-9$ ) calculated with IBM parameters listed in Table 1 as a function of the deformation parameter  $\beta$

region. We can see that in  $^{180-184}\text{W}$  nuclei a real prolate minimum ( $SU(3)$ -limit) occurs. The nucleus  $^{190}\text{W}$  ( $N = 116$ ) is proposed as a candidate for pure  $O(6)$  symmetry; in this nucleus the oblate and prolate minima coexist at close energies and are transformed into saddle points.

## CONCLUSIONS

The onset of transition from an axially symmetric rotor towards a  $\gamma$ -soft asymmetric rotor can be schematically described by breaking the  $SU(3)$  symmetry by the inclusion of a  $P^\dagger P$ . The  $^{180-190}\text{W}$  isotopic chain in the  $SU(3)$ - $O(6)$  direct region has been investigated. For these nuclei, the PESs have been calculated within framework of the IBM with intrinsic coherent formalism. The results indicate that the even-even  $^{180-190}\text{W}$  isotopes lie in the transition region  $SU(3)$ - $O(6)$ .

## REFERENCES

1. Iachello F., Arima A. The Interacting Boson Model. Cambridge: Cambridge Univ. Press, 1987.
2. Bohr A., Mottelson B. R. Nuclear Structure. V. II. New York: Benjamin, 1975.
3. Interacting Boson-Fermi System / Eds.: R. F. Casten, F. Iachello. New York: Plenum, 1981.
4. Cejar P. Landau Theory of Shape Phase Transitions in the Cranked Interacting Boson Model // Phys. Rev. Lett. B. 2003. V. 90. P. 112501.
5. Iachello F., Zamfir N. V. Quantum Phase Transitions in Mesoscopic Systems // Phys. Rev. Lett. 2004. V. 92. P. 212501.
6. Jolie J. et al. Triple Point of Nuclear Deformations // Phys. Lett. 2002. V. 89. P. 182502.

7. Arios J. M., Dukelsky J., Gracia-Ramos J. E. Quantum Phase Transitions in the Interacting Boson Model: Integrability, Level Repulsion, and Level Crossing // Phys. Rev. Lett. 2003. V. 91. P. 162502.
8. Iachello F. Dynamic Symmetries at the Critical Point // Phys. Rev. Lett. 2000. V. 85. P. 3580.
9. Iachello F. Analytic Description of Critical Point Nuclei in a Spherical-Axially Deformed Shape Phase Transition // Phys. Rev. Lett. 2001. V. 87. P. 052502.
10. Rowe D. J., Turner P. S. The Algebraic Collective Model // Nucl. Phys. A. 2005. V. 753, Nos. 1–2. P. 94–105.
11. Arias J. M. et al.  $U(5)$ – $O(6)$  Transition in the Interacting Boson Model and the  $E(5)$  Critical Point Symmetry // Phys. Rev. C. 2003. V. 68. P. 041302.R–041304.R.
12. Rowe D. J. Phase Transitions and Quasidynamical Symmetry in Nuclear Collective Models: I. The  $U(5)$ – $O(6)$  Phase Transitions in the IBM // Nucl. Phys. A. 2004. V. 745. P. 47–78.
13. Turner P. S., Rowe D. J. Phase Transitions and Quasidynamical Symmetry in Nuclear Collective Models: II. The Spherical Vibrator to Gamma-Soft Rotor Transitions in an  $SO(5)$ -Invariant Bohr Model // Nucl. Phys. A. 2005. V. 756. P. 333–355.
14. Hellemans V. et al. Phase Transition in the Configuration Mixed Interacting Boson Model,  $U(5)$ – $O(6)$  Mixing // Acta Phys. Polon. B. 2007. V. 38. P. 1599–1603.
15. Khalaf A. M., Awad T. M. A Theoretical Description of  $U(5)$ – $SU(3)$  Nuclear Shape Transitions in the Interacting Boson Model // Prog. Phys. 2013. V. 1. P. 7–11.
16. Khalaf A. M., Hamdy H. S., El Sawy M. M. Nuclear Shape Transition Using Interacting Boson Model with the Intrinsic Coherent State // Ibid. V. 3. P. 44–51.
17. Yu X. L., Liang-Zhu Mu, Haiqing Wei. Approach to the Rotation Driven Vibrational to Axially Rotational Shape Transition along the Yrast Line of a Nucleus // Phys. Lett. B. 2006. V. 633. P. 49–53.
18. Rosensteel G., Rowe D. J. Phase Transition and Quasidynamical Symmetry in Nuclear Collective Models: III. The  $U(5)$  to  $SU(3)$  Phase Transition in the IBM // Nucl. Phys. A. 2005. V. 759. P. 92–128.
19. Iachello F. Phase Transitions in Angle Variables // Phys. Rev. Lett. 2003. V. 91. P. 132502.
20. Bonatsos D. et al.  $Z(5)$ : Critical Point Symmetry for the Prolate to Oblate Nuclear Shape Phase Transition // Phys. Lett. B. 2004. V. 588. P. 172.
21. Gupta J. P. The Nuclear Structure of  $^{182-186}\text{W}$  in IBM-1 // Proc. of Intern. Symp. on Nucl. Phys., 2009.
22. Abu Mosleh S., Scholten O. A Description of Odd-Mass W Isotopes in the Interacting Boson–Fermion Model // Nucl. Phys. A. 2012. V. 878. P. 37–48.
23. Navratil P., Barrett B. R., Dobes J. M1 Properties of Tungsten Isotopes in the Interacting Boson Model-2 // Phys. Rev. C. 1996. V. 53. P. 2794.
24. Ginocchio J. N., Kirson M. W. An Intrinsic State for the Interacting Boson Model and Its Relationship to the Bohr–Mottelson Model // Nucl. Phys. A. 1980. V. 350. P. 31.
25. Hara K., Sun Y. Projected Shell Model and High-Spin Spectroscopy // Intern. J. Mod. Phys. E. 1995. V. 4. P. 637.
26. Casten R. F. Nuclear Structure from a Simple Perspective. Thomson Learning. Oxford Univ. Press, 1990.
27. Scholten O. Computer Code PHINT, KVI. Groningen, 1980.
28. Brookhaven National Nuclear Data Center NNDC. <http://www.nndc.bnl.gov/>.

Received on May 5, 2015.